Priyotomo et al. International Journal of Mechanical and Materials Engineering (2015) 10:17
DOI 10.1186/s40712-015-0046-7

International Journal of Mechanical and Materials Engineering
a SpringerOpen Journal

ORIGINAL ARTICLE Open Access

The environment-induced cracking of as-annealed $Ni_3(Si,Ti)$ and $Ni_3(Si,Ti)$ with 2Mo in sodium chloride solutions

Gadang Priyotomo[1*], Sanat Wagle[2], Kenji Okitsu[3], Akihiro Iwase[3], Yasuyuki Kaneno[3], Rokuro Nishimura[3] and Takayuki Takasugi[3]

Abstract

Background: The environment-induced cracking (EIC) of as-annealed $Ni_3(Si,Ti)$ and $Ni_3(Si,Ti)$ with 2Mo has been researched as functions of applied stress, chloride ion concentration, test temperature, and pH.

Methods: The investigation of EIC was carried out by applying a constant method in NaCl solutions.

Results: The EIC susceptibility of both intermetallic compounds increased with increasing test temperature and Cl^- ion concentration and increased with decreasing pH. The fracture surface morphologies of $Ni_3(Si,Ti)$ was intergranular while $Ni_3(Si,Ti)$ with 2Mo was a mixture of intergranular and transgranular, and the relationship between log t_f (time to failure) and log I_{ss} (steady-state elongation rate) became the identical straight line irrespective of applied stress, chloride ion concentration, test temperature, and pH, which means that I_{ss} becomes a relevant parameter for predicting t_f. The EIC susceptibility of $Ni_3(Si,Ti)$ with 2Mo was lower than that of $Ni_3(Si,Ti)$, which showed the advantageous effect of Mo.

Conclusions: From the results acquired, EIC of both the compounds was indicated to take place by hydrogen embrittlement (HE).

Keywords: Corrosion; Transgranular; Intermetallics; Hydrogen embrittlement; Environment-induced cracking; Intergranular

Background

$Ni_3(Si,Ti)$ intermetallic compounds with $L1_2$ structure have special strength and ductility properties, that is, (1) an increase in flow strength with increasing temperature and (2) high ductility over a wide range of test temperature (Takasugi et al. 1990; Takasugi and Yoshida 1991). Especially, their strength level was extraordinarily high compared to those of other $L1_2$ ordered intermetallic compounds which have been developed as advanced high temperature materials (Kaneno et al. 2008). On the other hand, $Ni_3(Si,Ti)$ intermetallic compounds have remarkable mechanical properties compared to those of conventional alloys such as nickel-based alloys and high-strength alloy steel and stainless steel. In addition, this intermetallic compound showed an excellent oxidation resistance in air at ambient and elevated operational temperatures (Kaneno and Takasugi 2007). Furthermore, an improvement in the mechanical property of the $Ni_3(Si,Ti)$ compound was also conducted with macro-alloying, i.e., addition of molybdenum, which enhanced hardness and tensile strength and improved elongation at various operational temperatures (Kaneno et al. 2011). Kaneno and co-workers (Kaneno et al. 2011) elucidated that both as-annealed $Ni_3(Si,Ti)$ and $Ni_3(Si,Ti)$ with 2Mo compounds after cold rolling then annealing at 1273 K in 1 h have higher ductilities compared with both as-cold rolled $Ni_3(Si,Ti)$ and $Ni_3(Si,Ti)$ with 2Mo, whereas the tensile stresses of both as-annealed $Ni_3(Si,Ti)$ and $Ni_3(Si,Ti)$ with 2Mo are lower than those of as-cold rolled $Ni_3(Si,Ti)$ and $Ni_3(Si,Ti)$ with 2Mo. On the other hand, the compounds have shown to be prone to environmental embrittlement (hydrogen embrittlement) at ambient temperature in moisture in air and hydrogen gas (Takasugi et al. 1993a; Takasugi et al. 1993b; Takasugi et al. 1995a). The addition

* Correspondence: gadangp@gmail.com
[1]Research Center for Metallurgy and Material, Indonesian Institute of Sciences, Kawasan PUSPIPTEK, Gd.474, Tangerang Selatan, Banten 15314, Indonesia
Full list of author information is available at the end of the article

of boron of $Ni_3(Si,Ti)$ was to restrain environmental embrittlement (Takasugi et al. 1995a), even though the intergranular attack was observed for this as-homogenized compound in acidic solutions, which took place by boron segregation at grain boundaries (Priyotomo et al. 2011).

Moreover, the other researchers already investigated the advantageous effect of Cr and Nb addition for reducing the susceptibility of hydrogen embrittlement for $Ni_3(Si,Ti)$ compound in air and distilled water, and H_2 gas (Takasugi and Hanada 2000; Ma et al. 1995; Kaneno et al. 2002) but not Mo addition. On the contrary, Priyotomo and co-workers found that the EIC susceptibility of as-cold rolled $Ni_3(Si,Ti)$ with the addition of Mo was lower than that of as-cold rolled $Ni_3(Si,Ti)$, which showed the beneficial effect of Mo (Priyotomo et al. 2015). Moreover, the usefulness of investigating the environment-induced cracking of as-annealed $Ni_3(Si,Ti)$ and $Ni_3(Si,Ti)$ with 2Mo shows the effect of Mo.

However, with regard to as-annealed $Ni_3(Si,Ti)$ and as-annealed $Ni_3(Si,Ti)$ with 2Mo compounds, there is little study on environment-induced cracking (EIC) in aqueous solution, Therefore, we have investigated the EIC behavior of those intermetallic compounds in chloride solutions as functions of applied stress, test temperature, chloride (Cl^-) ion concentration, and pH by applying a constant load method. The objectives of the paper are (1) to clarify the EIC behavior of those intermetallic compounds and (2) to presume an EIC mechanism.

Methods

Ni-11 at.% Si-9.5 at.% Ti and Ni-11 at.% Si-7.5 at.% Ti-2 at.% Mo compounds with the addition of 50 wt. ppm of boron were prepared by applying an arc-melting method under an argon gas atmosphere. Afterward, the ternary alloy will be written as $Ni_3(Si,Ti)$, and the quaternary alloys will be mentioned as $Ni_3(Si,Ti)$ with 2Mo. The chemical compositions of those materials are given in Table 1.

Those intermetallic compounds were homogenized at 1323 K for 2 days under an argon atmosphere and then cooled with a cooling rate of 283 K/min in a vacuum furnace. Homogenized ingot was conducted with a warm rolling at 573 K in open air until obtaining a certain thickness and then with a cold rolling until 1.2 mm of thickness in 75 % reduction. After that, the rolled ingot was annealed at 1273 K for 1 h under an argon atmosphere, where the ultimate tensile stress, yield stress, and strain of as-annealed $Ni_3(Si,Ti)$ were 1453 MPa, 673.2 MPa, and 42 %, while those of as-annealed $Ni_3(Si,Ti)$ with 2Mo were 1530 MPa, 840 MPa, and 35.5 %, respectively. Furthermore, the high strains of both intermetallic compounds mean that the compounds tended to the ductile materials. The effect of Ti addition increased a property of ductility for $Ni_3(Si,Ti)$ compounds (Kaneno et al. 2002) where the addition of Mo could slightly reduce the strain of $Ni_3(Si,Ti)$ with 2Mo compounds (Kaneno et al. 2011). In addition, the microstructure of as-annealed $Ni_3(Si,Ti)$ showed an $L1_2$ single phase with an equiaxed grain while as-annealed $Ni_3(Si,Ti)$ with 2Mo showed a very fine microstructure of equiaxed grain containing an $L1_2$ phase and a two-phase microstructure consisting of $L1_2$ and Ni_{ss} phases as well as Kaneno and co-workers' results (Kaneno et al. 2011).

Table 1 The chemical compositions of those prepared materials

Alloy	At.%											ppm
	C	Si	Mn	P	S	Ni	Cr	Mo	Al	Fe	Ti	B
$Ni_3(Si,Ti)$	–	11.0	–	–	–	79.5	–	–	–	–	9.5	50
$Ni_3(Si,Ti)$ + 2Mo	–	11.0	–	–	–	79.5	–	2	–	–	7.5	50

The specimens were manufactured (gauge length 10 mm, width 2 mm, and thickness 1.2 mm), where they were cut perpendicularly to the rolling direction. Prior to the experiments, the specimens were polished to 1000 grit emery paper, degreased with acetone in an ultrasonic cleaner, and then washed with distilled water. The test solution used was sodium chloride (NaCl) solution with various chloride ion concentrations (10^{-4}–2 kmol/m^3) prepared from distilled water and guaranteed grade reagent. The test temperature was in the range of 333–373 K with an accuracy of ±1 K. The pH was in the range of 2–8. All experiments were carried out under an open circuit condition.

A lever-type constant load apparatus (lever ratio 1:10) to which the specimens can be separately and simultaneously attached was used with a cooling system on top to avoid evaporation of the test solution during the experiments. The specimens set into the EIC cell were insulated from rod and grip by a surface oxidized zirconium tube. Elongation of the specimen under the constant load condition was measured by an inductive linear transducer with an accuracy of ±0.01 mm.

Results and discussion

Corrosion elongation curve and three parameters (t_f, l_{ss}, and t_{ss})

Figure 1 shows a representative of the corrosion curves (elongation versus time) up to failure for as-annealed $Ni_3(Si,Ti)$ at a constant applied stress of 1000 MPa and $Ni_3(Si,Ti)$ with 2Mo at a constant applied stress of 1450 MPa in 0.5 kmol/m^3 NaCl solution at 313 K. In addition, the result of corrosion elongation curves can be obtained, when a constant load is applied to a specimen at a constant temperature in corrosive environments and a time variation in elongation up to fracture (Nishimura 1990). They consisted of three time intervals with an initial rise of elongation, constant elongation,

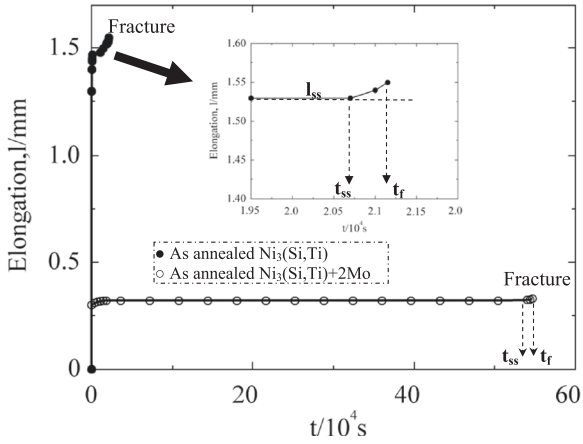

Fig. 1 Corrosion elongation curve of as-annealed $Ni_3(Si,Ti)$ at 1000 MPa and as-annealed $Ni_3(Si,Ti)$ + 2Mo at 1450 MPa in 0.5 kmol/m^3 NaCl solution at 313 K. t_f time to failure, l_{ss} steady-state elongation rate, t_{ss} transition time

and second rise in elongation to failure as well as those intervals for as-cold rolled $Ni_3(Si,Ti)$ and $Ni_3(Si,Ti)$ with 2Mo (Priyotomo et al. 2015). Furthermore, as shown in the magnified figure inserted in Fig. 1, the three parameters were acquired for each specimen at every applied stress: time to failure (t_f), steady-state elongation rate (l_{ss}) for the straight part of the corrosion elongation curve, and transition time (t_{ss}), where t_{ss} is the time when the elongation deviates from linearity. However, we could get only l_{ss} from the corrosion elongation curve, when it was not fractured within a laboratory time scale (<10^7 s).

Applied stress dependence of the three parameters

Figure 2 shows the relationship between applied stress and t_f in 0.5 kmol/m^3 NaCl solution at 313 K for both $Ni_3(Si,Ti)$ and $Ni_3(Si,Ti)$ with 2 Mo. The relationships were found to be divided into three regions (1–3 in Fig. 2), where arrows in region 3 mean that the specimens of $Ni_3(Si,Ti)$ were not fractured within a laboratory scale (<10^7 s) as well as those regions for as-cold rolled $Ni_3(Si,Ti)$ and $Ni_3(Si,Ti)$ with 2Mo (Priyotomo et al. 2015). In addition, in region 3, the specimen of $Ni_3(Si,Ti)$ had no fracture within a laboratory scale while that of $Ni_3(Si,Ti)$ + 2Mo was fractured within a laboratory scale. The maximum applied stress (σ_{max}) and the minimum stress (σ_{min}) in region 2 become larger for $Ni_3(Si,Ti)$ with 2Mo than those of $Ni_3(Si,Ti)$, and the t_f of $Ni_3(Si,Ti)$ was longer than that of $Ni_3(Si,Ti)$ in region 2.

Figure 3 shows the relationship between applied stress and l_{ss} for $Ni_3(Si,Ti)$ and $Ni_3(Si,Ti)$ with 2Mo in 0.5 kmol/m^3 NaCl solution at 313 K. It was also found that the relationships were divided into three regions (1–3 in Fig. 3), corresponding to those in Fig. 2. The steady-state elongation rate, l_{ss} of $Ni_3(Si,Ti)$ with 2Mo, was smaller than that of $Ni_3(Si,Ti)$ in region 2. Furthermore, in region 3, $Ni_3(Si,Ti)$ had no fracture with the order of 10^{-12} m/s while $Ni_3(Si,Ti)$ with 2Mo was fractured with the same order. Figure 4 shows the relationship between applied stress and t_{ss}/t_f for both $Ni_3(Si,Ti)$ and $Ni_3(Si,Ti)$ with 2Mo in 0.5 kmol/m^3 NaCl solution at 313 K. In region 1, the value of t_{ss}/t_f tended to increase with increasing applied stress and became close to unity for both intermetallic compounds, whereas that in region 2 was almost constant independent of applied stress with a high value of 0.98 ± 0.02. On the other hand, in region 3, the value of t_{ss}/t_f for $Ni_3(Si,Ti)$ could not be acquired, because no fracture took place, whereas the value of that for $Ni_3(Si,Ti)$ with 2Mo became close to unity.

The result thus obtained indicated that the applied stress dependence of the three parameters was basically

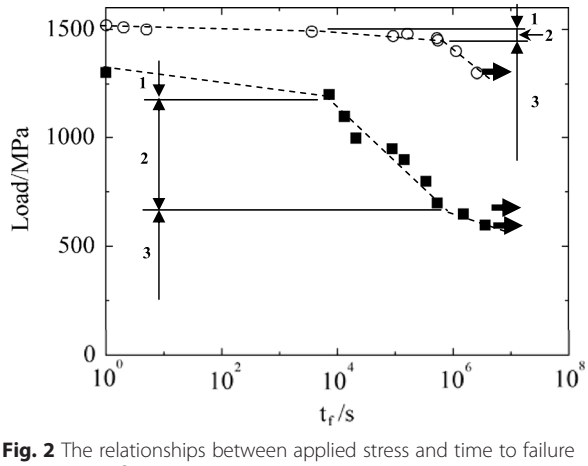

Fig. 2 The relationships between applied stress and time to failure in 0.5 kmol/m^3 NaCl solution at 313 K. $Ni_3(Si,Ti)$ (*black square*). $Ni_3(Si,Ti)$ with 2Mo (*circle*)

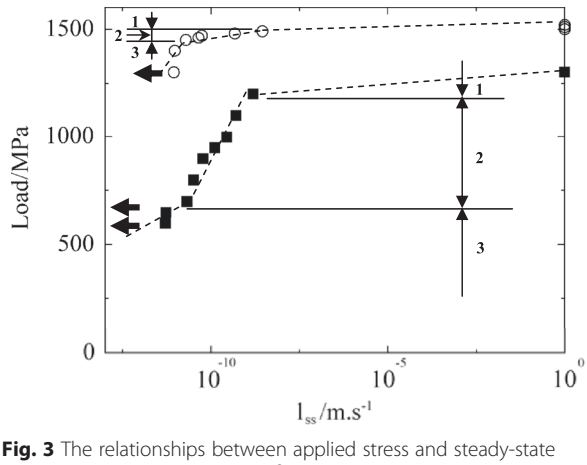

Fig. 3 The relationships between applied stress and steady-state elongation rate in 0.5 kmol/m^3 NaCl solution at 313 K. $Ni_3(Si,Ti)$ (*black square*). $Ni_3(Si,Ti)$with 2Mo (*circle*)

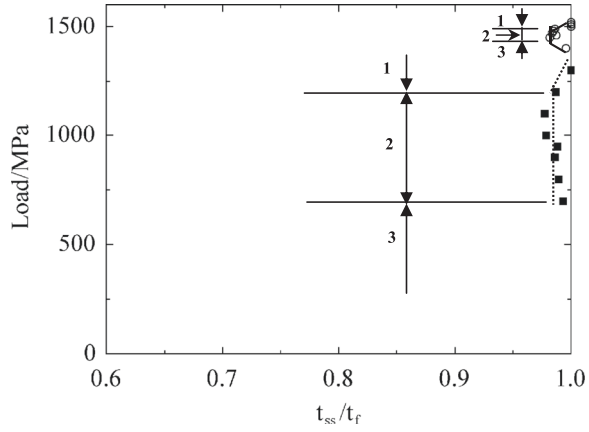

Fig. 4 The relationships between applied stress and ratio of transition time to time to failure in 0.5 kmol/m^3 NaCl solution at 313 K. Ni_3(Si,Ti) (*black square*). Ni_3(Si,Ti) with 2Mo (*circle*)

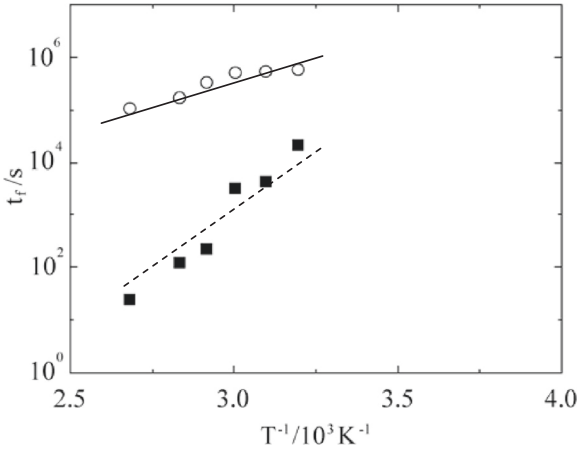

Fig. 5 The relationships between time to failure and a reciprocal of test temperature measured in 0.5 kmol/m^3 NaCl solution. Ni_3(Si,Ti) at a constant applied stress of 1000 MPa (*black square*). Ni_3(Si,Ti) with 2Mo at a constant applied stress of 1450 MPa (*circle*)

the same as those for as-cold rolled Ni_3(Si,Ti) and Ni_3(Si,Ti) with 2Mo (Priyotomo et al. 2015), austenitic stainless steel (Alyousif and Nishimura 2006; Alyousif and Nishimura 2007), Al-Cu alloy (Izumoto and Nishimura 2010), and pure Ti (Nishimura et al. 2008). Therefore, it was presumed that the three regions (1 to 3) for both as-annealed intermetallic compounds corresponded to the stress-dominated, EIC-dominated, and corrosion-dominated regions, respectively. The deviation of linearity each region could be applied to divides the three regions. Nishimura and co-worker elucidated that the stress corrosion cracking (SCC) occurrence could take place in the SCC-dominated region (Nishimura and Yamakawa 1998). In the stress-dominated and corrosion-dominated regions, the reduction in cross-sectional area is caused by high applied stress in any environments and by a general corrosion in the case of the intermediate and aggressive environments (Nishimura and Yamakawa 1998). Furthermore, the applied stress at the border between the EIC-dominated and corrosion-dominated regions is the minimum applied stress or threshold stress (σ_T), below which no EIC occurs.

Test temperature dependence of the three parameters

Figure 5 shows the relationship between t_f and a reciprocal of test temperature at a constant applied stress of 1000 MPa for Ni_3(Si,Ti) and at that of 1450 MPa for Ni_3(Si,Ti) with 2Mo in 0.5 kmol/m^3 NaCl solution, where these applied stresses belonged to those in the EIC-dominated region. On both intermetallic compounds, t_f increased linearly with increasing the reciprocal of test temperature over the whole temperature range carried out. In the same way, the l_{ss}-1/T relationship corresponded to that in Fig. 5 as shown in Fig. 6. Figure 7 shows the relationships between t_{ss}/t_f and a reciprocal of test temperature in the EIC-dominated region. The decrease in t_f and the increase in l_{ss} with an increase in the test temperature propose the contribution of corrosion reaction on the fracture of these compounds. It was found that t_{ss}/t_f for both those intermetallic compounds was almost constant independent of test temperature and was the same in that of the EIC-dominated region as shown in Fig. 4.

Chloride ion concentration dependence of the three parameters

Figure 8 shows the relationship between t_f and Cl^- ion concentration for Ni_3(Si,Ti) at a constant applied stress of 1000 MPa and Ni_3(Si,Ti) with 2Mo at 1450 MPa in

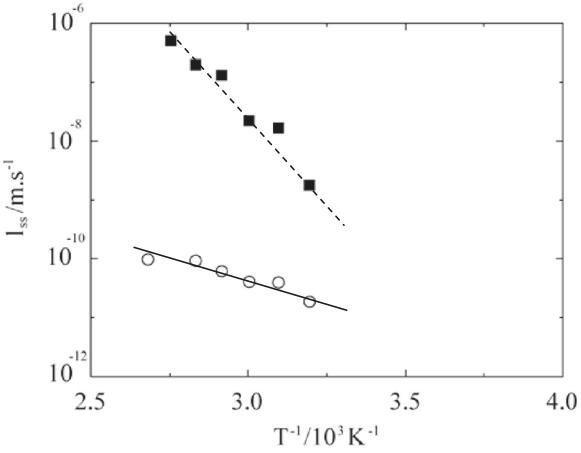

Fig. 6 The relationships between steady-state elongation rate and a reciprocal of test temperature measured in 0.5 kmol/m^3 NaCl solution. Ni_3(Si,Ti) at a constant applied stress of 1000 MPa (*black square*). Ni_3(Si,Ti) with 2Mo at a constant applied stress 1450 MPa (*circle*)

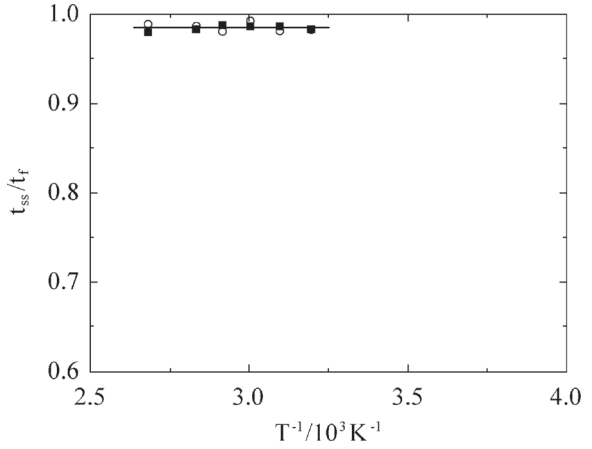

Fig. 7 The relationships between ratio of transition time to time to failure and a reciprocal of test temperature in the EIC-dominated region measured in 0.5 kmol/m^3 NaCl solution. $Ni_3(Si,Ti)$ at a constant applied stress of 1000 MPa (*black square*). $Ni_3(Si,Ti)$ with 2Mo at a constant applied stress of 1450 MPa (*circle*)

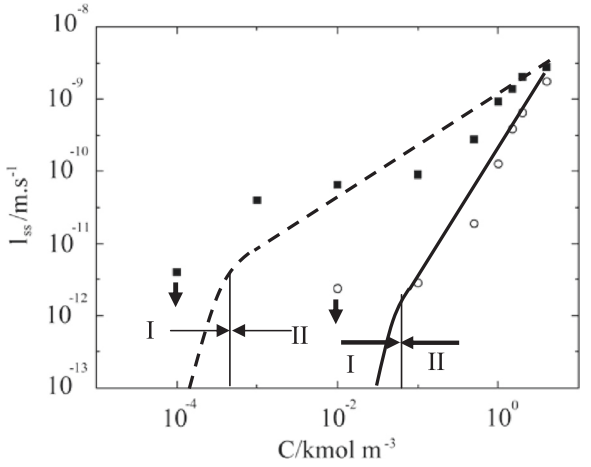

Fig. 9 The relationships between steady-state elongation rate and chloride ion concentration in NaCl solution at 313 K. $Ni_3(Si,Ti)$ at a constant applied stress of 1000 MPa (*black square*). $Ni_3(Si,Ti)$ with 2Mo at a constant applied stress of 1450 MPa (*circle*)

NaCl solutions for 313 K, where these applied stresses belonged to those in the EIC-dominated region. The relationship at each intermetallic compound was divided into two regions (I–II). On both compounds, in region I, no fracture occurred. In region II, t_f decreased with increasing Cl^- ion concentration. Moreover, the deviation of linearity each region could be applied to divides the two regions.

Figure 9 shows the relationship between l_{ss} and Cl^- ion concentration for $Ni_3(Si,Ti)$ at a constant applied stress of 1000 MPa and $Ni_3(Si,Ti)$ with 2Mo at 1450 MPa in NaCl solutions for 313 K. The Cl^- ion concentration dependence of l_{ss} corresponded to that of t_f in Fig. 8. Figure 10 shows the relationship between t_{ss}/t_f and Cl ion concentration for $Ni_3(Si,Ti)$ at a constant applied stress of 1000 MPa and $Ni_3(Si,Ti)$ with 2Mo at 1450 MPa in NaCl solutions for 313 K, where t_{ss}/t_f at region I could not be acquired when no fracture occurred. From Fig. 10, t_{ss}/t_f for both compounds was almost constant independent of Cl^- ion concentration in region II and was the same high value of 0.98 ± 0.02 as those in Figs. 4 and 7. Furthermore, in region I, the chloride concentrations at which longer fracture time occurred was defined as a critical chloride concentration (Cl^-_{cri}) where no fracture occurred within the laboratory time scale below the critical chloride

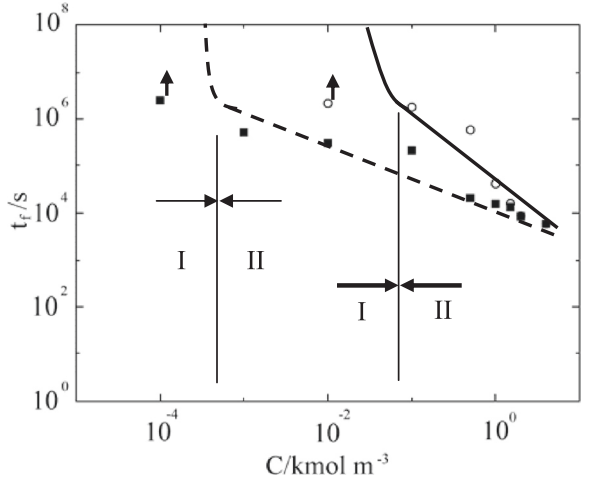

Fig. 8 The relationships between time to failure and chloride ion concentration in NaCl solution at 313 K. $Ni_3(Si,Ti)$ at a constant applied stress of 1000 MPa (*black square*). $Ni_3(Si,Ti)$ with 2Mo at a constant applied stress of 1450 MPa (*circle*)

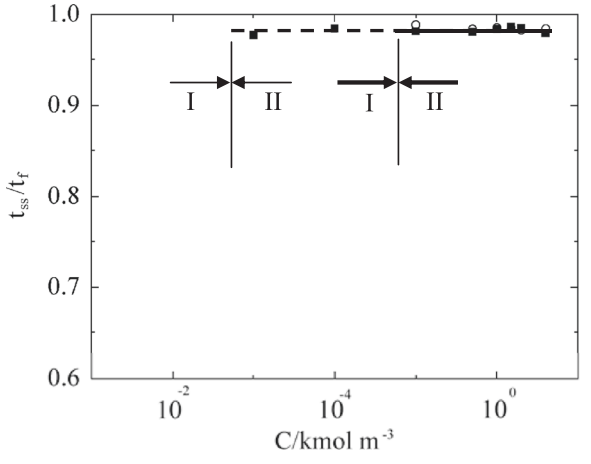

Fig. 10 The relationships between ratio of transition time to time to failure and chloride ion concentration in NaCl solution at 313 K. $Ni_3(Si,Ti)$ at a constant applied stress of 1000 MPa (*black square*). $Ni_3(Si,Ti)$ with 2Mo at a constant applied stress of 1450 MPa (*circle*)

concentration of both intermetallic compounds. The Cl^-_{cri} were found to be approximately 0.08 kmol/m^3 NaCl solution for Ni_3(Si,Ti) with 2Mo and 0.0007 kmol/m^3 NaCl solution for Ni_3(Si,Ti).

pH dependence of the three parameters

Figure 11 shows the relationship between t_f and pH in 0.5 kmol/m^3 NaCl solution at 313 K for Ni_3(Si,Ti) at a constant applied stress of 1000 MPa and Ni_3(Si,Ti) with 2Mo at 1450 MPa, where these applied stresses belonged to those in the EIC-dominated region. The relationship at each intermetallic compound was divided into three regions (A–C). On both compounds, in region A, t_f decreased rapidly with increasing pH. In region B, t_f slightly increased linearity with increasing pH, while in region C, no fracture occurred within the laboratory time scale. Moreover, the deviation of linearity each region could be applied to divides the three regions.

Figure 12 shows the relationship between l_{ss} and pH in 0.5 kmol/m^3 NaCl solution at 313 K for Ni_3(Si,Ti) at a constant applied stress of 1000 MPa and Ni_3(Si,Ti) with 2Mo at 1450 MPa at 313 K. The pH dependence of l_{ss} corresponded to that of t_f in Fig. 11. Figure 13 shows the relationship between t_{ss}/t_f and pH in 0.5 kmol/m^3 NaCl solution at 313 K for Ni_3(Si,Ti) at a constant applied stress of 1000 MPa and Ni_3(Si,Ti) with 2Mo at 1450 MPa at 313 K, where t_{ss}/t_f at region C could not be obtained when no fracture occurred. From Fig. 13, t_{ss}/t_f for both compounds was almost constant independent of pH in region B and was the same high value of 0.98 ± 0.02 as those in Figs. 4, 7, and 10. However, in region A, the value of t_{ss}/t_f tended to be close to unity.

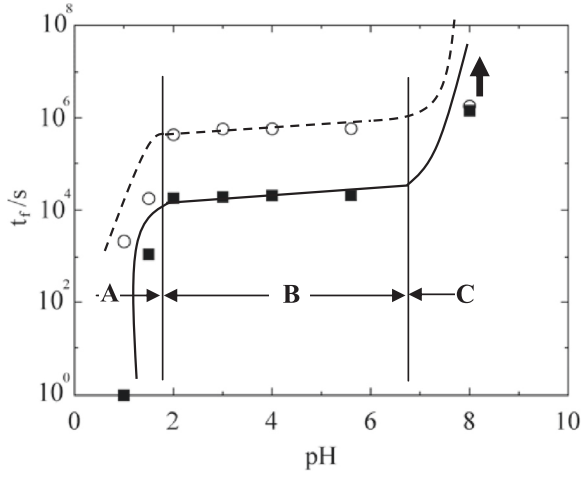

Fig. 11 The relationships between time to failure and pH in 0.5 kmol/m^3 NaCl solution at 313 K. Ni_3(Si,Ti) at a constant applied stress of 1000 MPa (*black square*). Ni_3(Si,Ti) with 2Mo at a constant applied stress of 1450 MPa (*circle*)

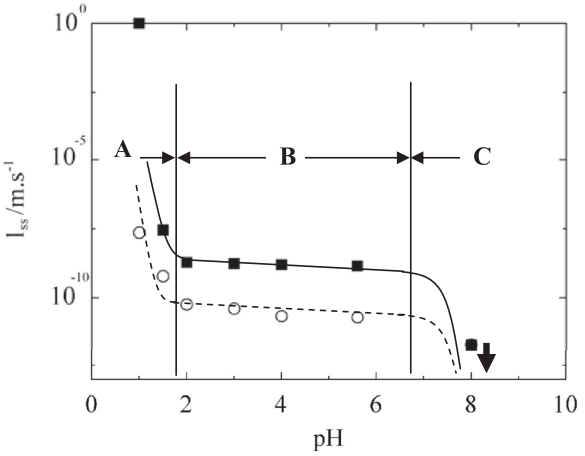

Fig. 12 The relationships between steady-state elongation rate and pH in 0.5 kmol/m^3 NaCl solution at 313 K. Ni_3(Si,Ti) at a constant applied stress of 1000 MPa (*black square*). Ni_3(Si,Ti) with 2Mo at a constant applied stress 1450 MPa (*circle*)

Fracture appearance

Figure 14 shows representative fracture appearances of Ni_3(Si,Ti) at a constant applied stress of 1000 MPa and Ni_3(Si,Ti) with 2Mo at 1450 MPa in 0.5 kmol/m^3 NaCl solution at 313 K. The fracture appearances of Ni_3(Si,Ti) were intergranular while Ni_3(Si,Ti) with 2Mo was a mixture of intergranular and transgranular. The same fracture appearance was observed for the specimens obtained in the experiments with the change in applied stress in the EIC-dominated region, test temperature, Cl^- ion concentration in region II, and pH in region B. On the other hand, applied stress dependence in regions 1 and 3 and pH in region A were predominantly dimple.

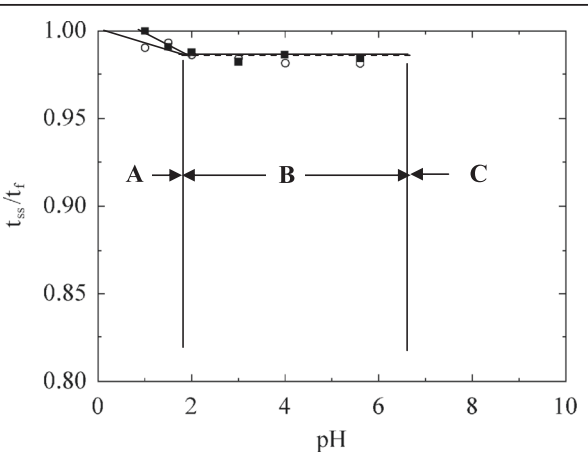

Fig. 13 The relationship between the ratio of transition time to time to failure and pH in 0.5 kmol/m^3 NaCl solution at 313 K. Ni_3(Si,Ti) at a constant applied stress of 1000 MPa (*black square*). Ni_3(Si,Ti) with 2Mo at a constant applied stress of 1450 MPa (*circle*)

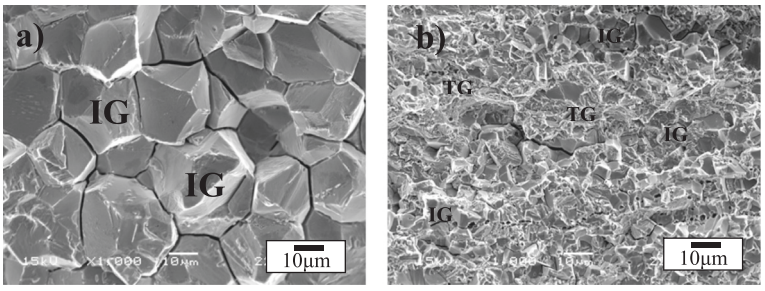

Fig. 14 The representative fracture appearances of **a** as-annealed $Ni_3(Si,Ti)$ at 1000 MPa and **b** as-annealed $Ni_3(S,Ti)$ with 2Mo at 1450 MPa in 0.5 kmol/m^3 NaCl solution at 313 K (in the EIC-dominated region)

In this work, we divided the results of the synergy of corrosion and mechanical stress for the as-annealed $Ni_3(Si,Ti)$ and $Ni_3(Si,Ti)$ with 2Mo into three regions 1–3 in applied stress dependence and A–C in pH dependence while in Cl^- ion concentration, the result of those for both intermetallic compounds divided into two regions I–II. The corrosive condition was fixed at 313 K in 0.5 kmol/m^3 NaCl solution, and the three regions were observed with increasing applied stress: No failure region 3 for $Ni_3(Si,Ti)$ and failure region 3 for $Ni_3(Si,Ti)$ with 2Mo where the mechanical stress and corrosiveness were too low to lead failure, region 2 where the mechanical stress became adequate to induce EIC at the given corrosiveness, and region 1 where the mechanical stress is too high to induce EIC at the given corrosiveness, with a consequent mechanical failure. This is defined as stress-dominated region. Moreover, the corrosiveness was changed from high to low by decreasing pH. Corrosion-dominated region is A, where corrosive degradation is too rapid in induced EIC at the applied mechanical stress, leading to final mechanical failure of the specimen, and final cross section is too small to avoid the mechanical failure whereas no corrosion-dominated region occurs in Cl^- ion concentration dependence. Regions II and B are the EIC region where both corrosiveness and mechanical stress act synergistically to induce EIC. In regions I and C, both mechanical stress and corrosiveness are too low to lead failure, while the chloride concentration of intermetallic compounds are below their critical chloride concentration in region I although material degradation proceeds by prolonged corrosion. As is well known, EIC occurs by the synergy of mechanical stress and corrosion in regions 2, II, and B. Therefore, let us elucidate the behavior of EIC of these intermetallic compounds.

A parameter for prediction of time to failure

Figure 15 shows the relationship between l_{ss} and t_f for $Ni_3(Si,Ti)$ and $Ni_3(Si,Ti)$ with 2Mo in the EIC-dominated region, acquired as functions of applied stress in the EIC-dominated region (Figs. 2 and 3), test temperature (Figs. 5 and 6), Cl^- ion concentration in region II (Figs. 8 and 9), and pH in region B (Figs. 11 and 12). The relationship was found to become an identical straight line regardless of applied stress, test temperature, Cl^- ion concentration, and pH as expressed below,

$$\mathrm{Log} l_{ss} = -1.2 \log t_f - 3.8 \quad (1)$$

The above linear equation means that l_{ss} is a relevant parameter for predicting t_f. In addition, it was found that the slope in Eq. (1) was the same as those for both as-cold rolled $Ni_3(Si,Ti)$ and $Ni_3(Si,Ti)$ with 2Mo (Priyotomo et al. 2015), Al-Cu alloy (Izumoto and Nishimura 2010), pure Ti (Nishimura et al. 2008), and austenitic stainless steels (Alyousif and Nishimura 2008). Furthermore, from the extrapolation of straight line to the t_f axis, when l_{ss} becomes of the order of 10^{-12} m/s, t_f has the order of 10^7 s, which is beyond the laboratory time scale. Therefore, whenever l_{ss} is of the order of 10^{-12} m/s or less, it is

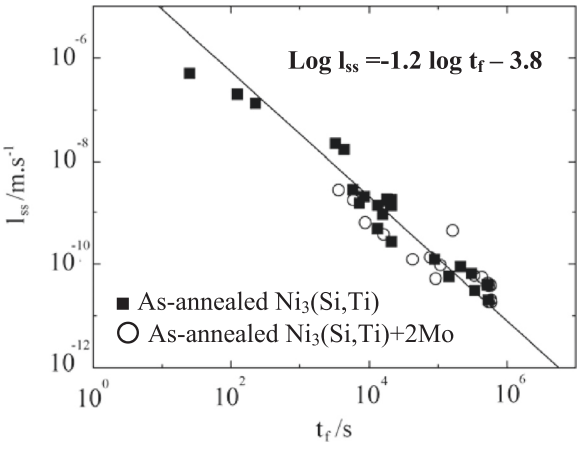

Fig. 15 The relationship between steady-state elongation rate and time to failure in the EIC-dominated region obtained as functions of applied stress, chloride ion concentration, test temperature, and pH for $Ni_3(Si,Ti)$ and $Ni_3(Si,Ti)$ with 2Mo

concluded that no failure occurs within the laboratory time scale. Therefore, this shows that l_{ss} is also an indicator on assessment of whether EIC takes place or not. As for the relationship between l_{ss} and t_f in region A (Figs. 11 and 12) for both intermetallic compounds and in region 3 (Figs. 2 and 3) for Ni_3(Si,Ti) with 2Mo, the relation deviated from Eq. (1), which means that the fracture did not occur by EIC.

Determination of SCC or hydrogen embrittlement

The results obtained showed that the EIC of both intermetallic compounds took place with an identical EIC mechanism from the following things: (1) the value of t_{ss}/t_f was always 0.98 ± 0.02; (2) the fracture appearances were intergranular for as-annealed Ni_3(Si,Ti) and the mixture of intergranular and transgranular; and (3) the relationship between log l_{ss} and log t_f was identical, irrespective of applied stress, test temperature, Cl^- ion concentration, and pH. Furthermore, EIC takes place by either SCC or hydrogen embrittlement (HE). Therefore, we will deduce which is the cause of EIC of these intermetallic compounds considering the present results and those previously reported.

A weight loss was investigated for both compounds in 0.5 kmol/m^3 NaCl solution at 313 K without applied stress, where the procedure and conditions were the same as those reported in those previous papers (Priyotomo et al. 2011; Priyotomo 2013; Priyotomo et al. 2012). It was found that the weight losses were not detected clearly and then the corrosion rate was negligibly small, although they were detected for both compounds in the low pH (region A in Fig. 11). This result corresponded to the fact that little change in surface appearance was observed before and after the EIC experiment with the same solution and test temperature under applied stress condition. In addition, we could not observe the presence of pits on the surface after the experiment. It is, thus, difficult to consider that SCC is responsible for EIC of these intermetallic compounds because SCC is induced by anodic reactions such as dissolution and film formation. For example, the SCC susceptibility of austenitic stainless steels (types 316 and 304) in chloride solutions decreased as pH increased and SCC did not occur at pH higher than 3 to 4 above which anodic reaction became negligible (Nishimura 1990).

For a possibility of HE occurrence, corrosion occurs slightly even in neutral NaCl solutions compared with in HCl solutions, even though we could not observe directly it as described above. However, the decrease of t_f with the rise in the test temperature as shown in the Arrhenius plots of Fig. 5 indicates the contribution of chemical reaction to EIC. Therefore, it is presumed that the anodic reactions such as dissolution (Eq.(2)) and formation of hydroxide (Eq.(3)) or oxide (Eq.(4)) would occur as follows:

$$Ni \rightarrow Ni^{2+} + H_2O \rightarrow Ni(OH)^+ + H^+ \quad (2)$$

$$Ni(OH)^+ + H_2O \rightarrow Ni(OH)_2 + H^+ \quad (3)$$

or

$$Ni(OH)^+ \rightarrow NiO + H^+ \quad (4)$$

where only Ni as the main element is taken into consideration for simplicity. At a very initial stage of corrosion reaction, dissolved oxygen contributes to cathodic reaction, whereas H^+ formed through Eqs. (2) to (4) would begin to be preferentially reduced after consumption of dissolved oxygen around the specimen surface. A part of H^+ would be reduced and the formation of H_{ad} and H_{ab} proceeds as expressed below,

$$H^+ + e^- \rightarrow H_{ad} \rightarrow H_{ab} \quad (5)$$

where H_{ad} is the adsorbed hydrogen and H_{ab} the absorbed hydrogen. A portion of H_{ab} would diffuse into the bulk and would cause an increase in the plasticity on a local scale as slip steps, which is defined hydrogen enhanced local plasticity (HELP) (Birnbaum and Sofronis 1994), and the other would be possible to lead to the formation of hydride (Asaoka et al. 2002; Honotani et al. 1985; Wayman and Smith 1971).

Takasugi and co-workers (Takasugi et al. 1995a; Takasugi et al. 1995b) have found that the fracture behavior of the intermetallic compounds was affected by the absorption of a small amount of hydrogen in moist atmosphere, which they defined HE. This may support that the EIC under the present experimental conditions takes place by HE. Furthermore, the high value of t_{ss}/t_f and the slope of the linear relationship between log l_{ss} and log t_f were close to those for both as-cold rolled Ni_3(Si,Ti) and Ni_3(Si,Ti) with 2Mo(Priyotomo et al. 2015), Al-Cu alloy (Izumoto and Nishimura 2010), pure Ti (Nishimura et al. 2008), austenitic stainless steel (Alyousif and Nishimura 2008), and that suffered HE. Furthermore, the high value of t_{ss}/t_f of 0.98 suggests that fracture mostly occurred by embrittlement without ductile failure after EIC in a part of specimen, which has been generally observed in SCC. In addition, both intermetallic compounds have very high ultimate strength with high strain in room temperature where their strains reduce in 0.5 kmol/m^3 NaCl solution under at a constant applied stress for 313 K. Therefore, it is also presumed that these compounds would have the HE susceptibility. From the above considerations, it is summarized that the EIC of those intermetallic compounds in this work takes place by HE.

The effect of Mo on EIC

From the results acquired in the previous section, it was found that the addition of Mo to as-annealed $Ni_3(Si,Ti)$ could reduce the EIC (HE) susceptibility as well as as-cold rolled $Ni_3(Si,Ti)$ with 2Mo(Priyotomo et al. 2015), although the straight line in Fig 15 indicates that the EIC of these two intermetallic compounds occurred by the same mechanism. Moreover, the addition of Mo have the advantageous effect on general corrosion and pitting corrosion of austenitic stainless steel such as type 316 through an enrichment of Mo in passive film (Montemor et al. 1999; Bastidas et al. 2002). The explanation of the difference in EIC (HE) susceptibility between these intermetallic compounds is as follows. For $Ni_3(Si,Ti)$ with 2Mo, the amount of Mo was found to be more enriched in a mixture of $L1_2$ and fcc Ni than in the $L1_2$ phase (Priyotomo et al. 2012) while an oxide was distributed uniformly on the surface where no amount of Mo was distributed on the surface of $Ni_3(Si,Ti)$ (Priyotomo et al. 2011). Therefore, it is supposed that the general corrosion rate of $Ni_3(Si,Ti)$ would be reduced by the addition of Mo due to the formation of a more stable and adherent film containing with oxide, which correlates to the decrease in the magnitude of anodic and cathodic reactions. This means that the amount of absorbed hydrogen (H_{ab}) decreases and as a result, HE susceptibility is minimized. This present concept would be used to the results acquired as functions of test temperature, pH, and Cl^- ion concentration, that is, the corrosion rate increases with increasing test temperature and Cl^- ion concentration and decreases with increasing pH.

Conclusions

The EIC behavior of as-annealed $Ni_3(Si,Ti)$ and $Ni_3(Si,Ti)$ with 2Mo in NaCl solutions was investigated as functions of applied stress, test temperature, Cl^- ion concentration, and pH by applying the constant load method. The results obtained were concluded as follows:

1. From the applied stress dependence of the three parameters (t_f, l_{ss}, and t_{ss}), it was divided into three regions: the stress-dominated, EIC (HE)-dominated, and corrosion-dominated regions, respectively. Whenever EIC (HE) took place, the ratio of t_{ss}/t_f in the EIC (HE)-dominated region was held in a constant high value of 0.98 independent of applied stress, test temperature, Cl^- ion concentration, and pH. This is a fine indicator for the evaluation that EIC took place by HE.
2. The EIC susceptibility of both intermetallic compounds increased with increasing test temperature and chloride ion concentration and increased with decreasing pH.
3. The Mo addition substituting a portion of Ti in as-annealed $Ni_3(Si,Ti)$ was advantageous in minimizing the EIC susceptibility.
4. The relationship between time to failure (t_f) and steady-state elongation rate (l_{ss}) with the EIC occurrence region for both intermetallic compounds became an identical straight line irrespective of applied stress, test temperature, Cl^- ion concentration, and pH, which means that the steady-state elongation rate (l_{ss}) is the relevant parameter for the prediction of time to failure (t_f).
5. On the basis of the results, the EIC of both intermetallic compounds was presumed to take place by HE.

Competing interests

The authors declare that they have no competing interests.

Authors' contributions

GP carried out enviroment-induced cracking studies, participated in the sequence alignment, and drafted the manuscript. SW assisted for making the specimens. KO, AI, YK, RN and TT contributed to provide GP for apparatus of all experiments. All authors read and approved the final manuscript.

Author details

[1]Research Center for Metallurgy and Material, Indonesian Institute of Sciences, Kawasan PUSPIPTEK, Gd.474, Tangerang Selatan, Banten 15314, Indonesia. [2]Department of Physics and Technology, UiT The Arctic University of Norway, Tromsø 9037, Norway. [3]Department of Materials Science, Graduate School of Engineering, Osaka Prefecture University, 1-1, Gakuen-cho, Sakai, Osaka 599-8531, Japan.

Received: 30 April 2015 Accepted: 19 July 2015
Published online: 01 August 2015

References

Alyousif, MO, & Nishimura, R. (2006). The effect of test temperature on SCC behavior of austenitic stainless steels in boiling saturated magnesium chloride solution. *Corrosion Science, 48*, 4283–4293.

Alyousif, MO, & Nishimura, R. (2008). On the stress corrosion cracking and hydrogen embrittlement of sensitized austenitic stainless steels in boiling saturated magnesium chloride solutions: effect of applied stress. *Corrosion Science, 50*, 2919–2926.

Alyousif, MO, & Nishimura, R. (2007). The stress corrosion cracking behavior of austenitic stainless steels in boiling magnesium chloride solutions. *Corrosion Science, 49*, 3040–3051.

Asaoka, K, Yokoyama, K, & Nagumo, M. (2002). Hydrogen embrittlement of nickel–titanium alloy in biological environment. *Metall Mater Trans A, 33A*, 495–501.

Bastidas, JM, Torres, CL, & Polo, JL. (2002). Influence of molybdenum on passivation of polarised stainless steels in a chloride environment. *Corrosion Science, 44*, 625–633.

Birnbaum, HK, & Sofronis, P. (1994). Hydrogen-enhanced localized plasticity—a mechanism for hydrogen-related fracture. *Materials Science and Engineering: A, 176*, 191–202.

Honotani, S, Ohmori, Y, & Terasaki, F. (1985). Effect of nickel on hydride formation and hydrogen embrittlement in Ni-Cr-Fe alloys. *Materials Science and Engineering, 74*, 119–131.

Izumoto, E, & Nishimura, R. (2010). Environment-induced cracking of Al–Cu alloy (AA2017P-T3) under constant load in distilled water and sodium chloride solutions. *Corrosion Science, 53*, 886–893.

Kaneno, Y, Myoki, T, & Takasugi, T. (2008). Tensile properties of $L1_2$ intermetallic foils fabricated by cold rolling. *International Journal of Materials Research, 99*(11), 1229–1236.

Kaneno, T, & Takasugi, T. (2007). The effects of Nb and Cr addition on mechanical and chemical properties of cold-rolled $Ni_3(Si, Ti)$ intermetallic foils. *Materials Science Forum, 561–565*(1), 411–414.

Kaneno, Y, Fujimoto, Y, Yoshida, M, & Takasugi, T. (2011). Alloying effect on microstructure and mechanical properties of thermomechanically processed Ni_3(Si,Ti) alloys. *Journal of Materials Research, 102*(5), 1–7.

Kaneno, Y, Nakaaki, I, & Takasugi, T. (2002). Texture evolution during cold rolling and recrystallization of $L1_2$-type ordered Ni_3(Si,Ti) alloy. *Intermetallics, 10*(7), 692–700.

Ma, CL, Takasugi, T, & Hanada, S. (1995). The influence of chromium addition on the environmental embrittlement of Ni_3(Si,Ti) alloys at ambient temperatures. *Scripta Metallurgica et Materialia, 32*(7), 1025–1029.

Montemor, MF, Simoes, AMP, & Ferreira, MGS. (1999). The role of Mo in the chemical composition and semiconductive behaviour of oxide films formed on stainless steels. *Corrosion Science, 41*, 17–34.

Nishimura, R, & Yamakawa, K. (1998). Life prediction on SCC of solution annealed stainless steels under laboratory conditions. *Nuclear Engineering and Design, 182*, 165–173.

Nishimura, R. (1990). SCC failure prediction of austenitic stainless steels in acid solutions—effect of pH, anion species, and concentration. *Corrosion, 46*(4), 311–318.

Nishimura, R, Shirono, J, & Jonokuchi, A. (2008). Hydrogen-induced cracking of pure titanium in sulphuric acid and hydrochloric acid solutions using constant load method. *Corrosion Science, 50*, 2691–2697.

Priyotomo, G. (2013). The effect of annealing temperature after thermomechanical process to the corrosion behavior of Ni_3(Si, Ti) in chloride solution. *Teknologi Indonesia, 36*(2), 97–104.

Priyotomo, G, Okitsu, K, Iwase, A, Kaneno, Y, Nishimura, R, & Takasugi, T. (2011). The corrosion behavior of intermetallic compounds Ni_3(Si, Ti) and Ni_3(Si, Ti) + 2Mo in acidic solutions. *Applied Surface Science, 257*(19), 8268–8274.

Priyotomo, G, Wagle, S, Okitsu, K, Iwase, A, Kaneno, Y, Nishimura, R, & Takasugi, T. (2012). The corrosion behavior of Ni_3(Si, Ti) intermetallic compounds with Al, Cr, and Mo in various acidic solutions. *Corrosion Science, 60*, 10–17.

Priyotomo, G, Wagle, S, Okitsu, K, Iwase, A, Kaneno, Y, Nishimura, R, & Takasugi, T. (2015). The environment-induced cracking of as-cold rolled Ni_3(Si, Ti) and Ni_3(Si, Ti) with 2Mo in sodium chloride solutions. *Journal of Alloys and Compounds, 639*, 504–510.

Takasugi, T, Nagashima, M, & Izumi, O. (1990). Strengthening and ductilization of Ni_3Si by the addition of Ti elements. *Acta Metallurgica Et Materrialia, 38*, 747–755.

Takasugi, T, & Yoshida, M. (1991). Mechanical properties of Ni_3(Si, Ti) polycrystals alloyed with substitutional additions. *Journal of Materials Science, 26*, 3517–3525.

Takasugi, T, Nakayama, T, & Hanada, S. (1993a). Environmental embrittlement of Ni_3(Si, Ti) single crystals. *Materials Transactions JIM, 34*(9), 775–785.

Takasugi, T, Hono, K, Suzuki, S, Hanada, S, & Sakurai, T. (1993b). Environmental embrittlement and grain boundary segregation of boron in Ni_3(Si, Ti) and Co_3Ti alloys. *Scripta Metallurgica et Materiala, 9*(12), 1587–1591.

Takasugi, T, Ma, CL, & Hanada, S. (1995a). Environmental embrittlement and grain boundary segregation of boron and carbon in Ni_3(Si, Ti) alloys. *Materials Science and Engineering A, 192*(193), 407–412.

Takasugi, T, & Hanada, S. (2000). The effect of Nb addition on environmental embrittlement of a Ni_3(Si, Ti) alloy. *Intermetallics, 8*, 47–52.

Takasugi, T, Misawa, T, & Saitoh, H. (1995b). Effect of hydrogen—solute interaction on the environmental embrittlement of ordered intermetallics. *Materials Science and Engineering: A, 192*(193), 413–419.

Wayman, ML, & Smith, GC. (1971). Hydride formation in nickel-iron alloys. *Journal of Physics and Chemistry of Solids, 32*, 103–108.